© 2016. Published by The Company of Biologists Ltd | Development (2016) 143, 181 doi:10.1242/dev.133934

CORRECTION

Bicaudal C1 promotes pancreatic NEUROG3+ endocrine progenitor differentiation and ductal morphogenesis

Laurence A. Lemaire, Joan Goulley, Yung Hae Kim, Solenne Carat, Patrick Jacquemin, Jacques Rougemont, Daniel B. Constam and Anne Grapin-Botton

There were errors published in Development **142**, 858-870.

In the supplementary information, the sequences of four of the primers shown in Table S2 were incorrect. The correct sequences of these primers are as follows (5′-3′):

Hes1 mRNA reverse primer, gcgcggtatttccccaaca;

Onecut1 mRNA forward primer, agttccagcgcatgtcgg;

Onecut1 mRNA reverse primer, tttttgggggtgttgcctct;

Tcf7 mRNA reverse primer, agttcatagtacttggcctgctcttc.

The authors apologise to readers for these mistakes.

© 2015. Published by The Company of Biologists Ltd | Development (2015) 142, 858-870 doi:10.1242/dev.114611

RESEARCH ARTICLE

STEM CELLS AND REGENERATION

Bicaudal C1 promotes pancreatic NEUROG3+ endocrine progenitor differentiation and ductal morphogenesis

Laurence A. Lemaire[1,2], Joan Goulley[2], Yung Hae Kim[1,2], Solenne Carat[3], Patrick Jacquemin[4], Jacques Rougemont[3], Daniel B. Constam[2] and Anne Grapin-Botton[1,2,*]

ABSTRACT

In human, mutations in bicaudal C1 (BICC1), an RNA binding protein, have been identified in patients with kidney dysplasia. Deletion of *Bicc1* in mouse leads to left-right asymmetry randomization and renal cysts. Here, we show that BICC1 is also expressed in both the pancreatic progenitor cells that line the ducts during development, and in the ducts after birth, but not in differentiated endocrine or acinar cells. Genetic inactivation of *Bicc1* leads to ductal cell over-proliferation and cyst formation. Transcriptome comparison between WT and *Bicc1* KO pancreata, before the phenotype onset, reveals that PKD2 functions downstream of BICC1 in preventing cyst formation in the pancreas. Moreover, the analysis highlights immune cell infiltration and stromal reaction developing early in the pancreas of *Bicc1* knockout mice. In addition to these functions in duct morphogenesis, BICC1 regulates NEUROG3$^+$ endocrine progenitor production. Its deletion leads to a late but sustained endocrine progenitor decrease, resulting in a 50% reduction of endocrine cells. We show that BICC1 functions downstream of ONECUT1 in the pathway controlling both NEUROG3$^+$ endocrine cell production and ductal morphogenesis, and suggest a new candidate gene for syndromes associating kidney dysplasia with pancreatic disorders, including diabetes.

KEY WORDS: Embryo, Pancreas, Progenitors, Endocrine, Beta cell, Insulin, Diabetes, Differentiation, RNA-binding protein, Cysts, MODY5

INTRODUCTION

The pancreas is an endoderm-derived organ with dual functions. Acini have a digestive role and secrete enzymes reaching the duodenum through a network of ducts. The other function is endocrine; the islets of Langerhans secrete several hormones, including glucagon and insulin, that control blood glucose homeostasis. The destruction or functional impairment of the beta cells producing insulin (INS) leads to glucose intolerance and eventually diabetes. The etiology of type 2 and type 1 diabetes is multifactorial, including both environmental and genetic components. However, rare forms of diabetes are monogenic and give clues about beta cell physiology and formation. Indeed, mutations in genes involved in insulin production or secretion, such as glucokinase, *GLUT2* and *INS* itself, lead to mellitus diabetes. Other mutations affect genes involved in beta cell formation during embryogenesis (Ashcroft and Rorsman, 2012).

In mouse, pancreas formation starts around 8.5 days after fertilization (E8.5) with the specification of two regions of the foregut expressing PDX1 and HNF1B (Gu et al., 2002; Haumaitre et al., 2005). Both regions grow and bud into the surrounding mesenchyme. The epithelial cells of the buds will rearrange to form a pancreatic tree at around E12.5 (Kesavan et al., 2009; Pan and Wright, 2011). Prior to this, the bud comprises predominantly multipotent pancreatic progenitors, some of which have already progressed to endocrine progenitors and beyond to alpha cells. Thereafter, the so-called secondary transition starts. Cells located at the tip of the tree differentiate into acini, whereas the progenitor cells lining the ducts, expressing SOX9, PDX1, HNF1B and ONECUT1 (also called HNF6), restrict their potency to give rise to either functional ductal cells or to neurogenin3 (NEUROG3)-expressing endocrine progenitors (Seymour et al., 2012; Shih et al., 2012). The latter delaminate and differentiate into the five types of endocrine cells: beta cells, alpha cells secreting glucagon, delta cells secreting somatostatin, PP cells secreting pancreatic polypeptide and epsilon cells secreting ghrelin (GHRL) (Gradwohl et al., 2000). These cells cluster and form the islets of Langerhans at late gestation and during the first weeks after birth (Pan and Wright, 2011).

Monogenic diabetes is often a multi-organ disorder, sometimes comprising renal defects, as for example in Ivemark's syndrome (Ivemark et al., 1959; Vankalakunti et al., 2007), ciliopathies like Bardet–Biedl and Alström syndromes (Green et al., 1989; Marshall et al., 2005; Kousta et al., 2009), or some cases of neonatal permanent diabetes with hypothyroidism, in which *Glis3*, a transcriptional activator of *Neurog3*, is mutated (Taha et al., 2003; Senée et al., 2006). Maturity onset diabetes of the young 5 (MODY5) is a more frequent syndrome associated with diabetes and renal defects. MODY5 patients are characterized by mutations in *HNF1B* (Horikawa et al., 1997; Bingham and Hattersley, 2004). Although the human mutations have not been engineered into the mouse, whole-gene deletions in humans result in more severe phenotypes than those seen in mouse heterozygous *Hnf1b* loss-of-function (Ulinski et al., 2006). Zygotic *Hnf1b* deletion is lethal due to extra-embryonic tissue defects. Later mosaic or organ-specific inactivation of *Hnf1b* leads to pancreas agenesis or kidney cyst formation (Barbacci et al., 1999; Gresh et al., 2004; Haumaitre et al., 2005). Gene inactivation in mice suggests that other genes are also involved in both endocrine cell biogenesis and cyst prevention. Deletion of *Onecut1*, a regulator of *Hnf1b*, or late inactivation of *Sox9* both lead to endocrine cell decrease due to a failure to produce endocrine progenitors and cyst formation in the pancreas (Jacquemin et al., 2000; Shih et al., 2012).

Cyst formation is often a shared feature of kidney and pancreas pathologies. Indeed, inactivation of several genes, such as polycystic kidney disease 1 and 2 (*Pkd1* and *Pkd2*), causes cysts both in the

[1]DanStem, University of Copenhagen, 3B Blegdamsvej, Copenhagen N DK-2200, Denmark. [2]ISREC, Life Sciences, Ecole Polytechnique Fédérale de Lausanne, Lausanne CH-1015, Switzerland. [3]BBCF, Life Sciences, Ecole Polytechnique Fédérale de Lausanne, Lausanne CH-1015, Switzerland. [4]de Duve Institute, Université catholique de Louvain, Brussels B-1200, Belgium.

*Author for correspondence (anne.grapin-botton@sund.ku.dk)

Received 20 June 2014; Accepted 21 December 2014

Development (2015) 142, 858-870 doi:10.1242/dev.114611

kidneys and the pancreas without reported endocrine defects (Lu et al., 1997; Wu et al., 2000). Both genes are the main cause of autosomal dominant polycystic kidney disease (Reeders et al., 1985; Fossdal et al., 1993). Other mouse models of polycystic kidney diseases, including the *jcpk/jcpk* mouse, carry point mutations in *Bicc1* (Nauta et al., 1993; Flaherty et al., 1995; Cogswell et al., 2003). Its targeted inactivation causes left-right randomization and kidney cysts (Maisonneuve et al., 2009; Tran et al., 2010). Moreover, *BICC1* mutations have been identified in pediatric patients with kidney dysplasia (Kraus et al., 2012). BICC1 is a conserved RNA-binding protein with versatile functions (Mahone et al., 1995; Wessely et al., 2001; Gamberi and Lasko, 2012). In *Drosophila melanogaster*, it regulates *oskar* mRNA localization involved in anterio-posterior axis establishment (Saffman et al., 1998). In vertebrates, it can either promote or inhibit translation. Indeed, it blocks translational repression of *Pkd2* mRNA by miR-17, thereby stabilizing *Pkd2* mRNA levels (Tran et al., 2010). By contrast, it can promote repression of mRNA translation by targeting miR-125a to *Ac6* mRNA and miR-27a to *Pkia* mRNA (Piazzon et al., 2012). In ADPKD patients and in animal models, downregulation of *Pkd2* and elevated cAMP signaling promote cyst formation (Harris and Torres, 2009; Rees et al., 2014).

Based on the existence of syndromes combining pancreatic and renal defects and the role of BICC1 in the kidney, we investigated its possible function in the pancreas of mice. We found that *Bicc1* deletion leads to the formation of cysts exhibiting over-proliferation of ductal cells following *Pkd2* downregulation. Moreover, endocrine cells are decreased due to the repression of the endocrine progenitor gene *Neurog3*. We finally show that BICC1 functions downstream of *Onecut1*, a gene that also controls duct morphogenesis and endocrine-cell differentiation.

RESULTS

BICC1 is expressed in the pancreas progenitors and ducts during pancreas development

To investigate a possible role for BICC1 during embryonic pancreas formation, its expression was analyzed at different stages. *Bicc1* mRNA was already detected by qPCR at E10.5 (supplementary material Fig. S1A), whereas the protein was first detected at low levels at E11.5. The expression level increased over time, and it was still detected at E18.5 and after birth in ductal cells but not in beta cells (Fig. 1A-H; supplementary material Fig. S1D-I). At earlier stages, its expression was restricted to the pancreatic progenitors lining ducts and to a subset of NEUROG3$^+$ endocrine progenitors, mostly in those that had not yet delaminated to form islets. It was excluded from the endocrine cells and acini (Fig. 1I-T). As previously described in cell lines (Maisonneuve et al., 2009; Tran et al., 2010), BICC1 was present in the cytoplasm (Fig. 1I-K). BICC1 was also expressed at E11.5 in the hepatic main duct but not in the hepatoblasts (supplementary material Fig. S1B,C).

Bicc1 KO progenitor-lined ducts expand and form cysts

To further analyze the function of BICC1 during pancreas development, the pancreas from *Bicc1* KO mice was analyzed at different stages of development. Progressively expanding cysts lined by pancreatic progenitors were detected from E14.5 (Fig. 2A,B), confirming previous observations made at P1 in another *Bicc1* KO line and in *jcpk/jcpk* mouse model (Flaherty et al., 1995; Tran et al., 2010). The cysts were not a consequence of the left/right asymmetry defects seen in *Bicc1* KO, as they occurred both in left- and right-turned pancreata. Optical coherence microscopy (Villiger et al., 2009) revealed that the enlarged ducts formed an interconnected web rather than closed sacs (supplementary material Movies 1 and 2). The cystic web arose in the main duct and interlobular ducts, whereas the intercalated ducts were not enlarged. Quantification of ductal cells expressing dolichos biflorus agglutinin (DBA) at P0 revealed twice as many cells in *Bicc1* KO pancreata than in wild-type (WT) pancreata (Fig. 2C). Proliferating ductal cell quantification at E18.5 revealed a 1.5-fold increase in the proliferation index in *Bicc1* KO pancreata (Fig. 2D). However, it was not the primary cause of cyst formation, as proliferation of pancreatic progenitors at E14.5 was not affected by *Bicc1* deletion (Fig. 2E). Although rare, apoptotic cells were detected by terminal deoxynucleotidyl transferase-dUTP nick end labeling assay (TUNEL) in *Bicc1* KO ducts but not in WT ducts (Fig. 4A-C). Although sporadic cells positive for acinar markers and negative for ductal markers were found lining the cyst, we did not detect acinar to ductal metaplasia. The boundary between acinar and ductal compartments thus appears to be generally conserved (supplementary material Fig. S2A-D). Numerous cilia mutants form ductal cysts in the pancreas (Cano et al., 2004, 2006), and other cystic mutants have cilia defects (Pierreux et al., 2006; Kang et al., 2009), thus propounding that cilia defects might contribute to cyst formation in *Bicc1* KOs. However, at the beginning of cyst formation, cilia were present at E14.5 in *Bicc1* KOs and did not show any obvious defects (supplementary material Fig. S2E,F). Moreover, the number of cilia in both *Bicc1* KO cystic and non-cystic ducts at E18.5 was not affected (Fig. 2F-R). Taken together, these results show that BICC1 deficiency leads to cyst formation during development, and it is associated with increased ductal proliferation at later stages.

Endocrine cells are decreased in *Bicc1* KO pancreas

To further explore the role of BICC1 in the pancreas, we investigated the differentiation of the endocrine cell types. In *Bicc1* KO, islet architecture was disturbed at P0. The islets, detected by their immmunoreactivity for insulin (INS), glucagon (GCG) and somatostatin (SST), were visibly smaller. Many endocrine cells were scattered rather than clustered into islets (supplementary material Fig. S3A-F). A higher number of endocrine cells had not delaminated from the duct (supplementary material Fig. S3G-K).

At E14.5, the number of both alpha and beta cells, identified by their secreted hormones GCG and INS, respectively, were not changed (Fig. 3A-C). As the other endocrine cell types form a rare population, they were only analyzed at a later stage. At the end of gestation, the number of beta cells was reduced by 50%. The number of GHRL$^+$ cells (epsilon cells), SST$^+$ cells (delta cells) and PP$^+$ cells (PP cells) were all significantly decreased in *Bicc1* KO pancreata, to the same extent as the beta cells. Finally, the alpha cell number was reduced by 20% (Fig. 3D-F). *Bicc1* deletion thus leads to a global but late endocrine cell decrease during pancreas development.

NEUROG3$^+$ cells are reduced upon *Bicc1* deletion

Endocrine cell decrease might have different causes, such as reduced proliferation, dying cells or defective differentiation. Beta cell proliferation was quantified at E18.5, as endocrine proliferation was too low to be reliably quantified earlier. The percentage of beta cells expressing MKI67, also known as Ki67, was not changed in *Bicc1* KO pancreas compared with WT (Fig. 4D). Moreover, a TUNEL assay, performed at E18.5, showed no apoptosis in both WT and KO beta cells (Fig. 4A-C). To explore the possibility of a defect in the differentiation pathway we quantified the pancreatic progenitors and the NEUROG3$^+$ endocrine progenitor cells they produce. At E14.5, the number of

Development (2015) 142, 858-870 doi:10.1242/dev.114611

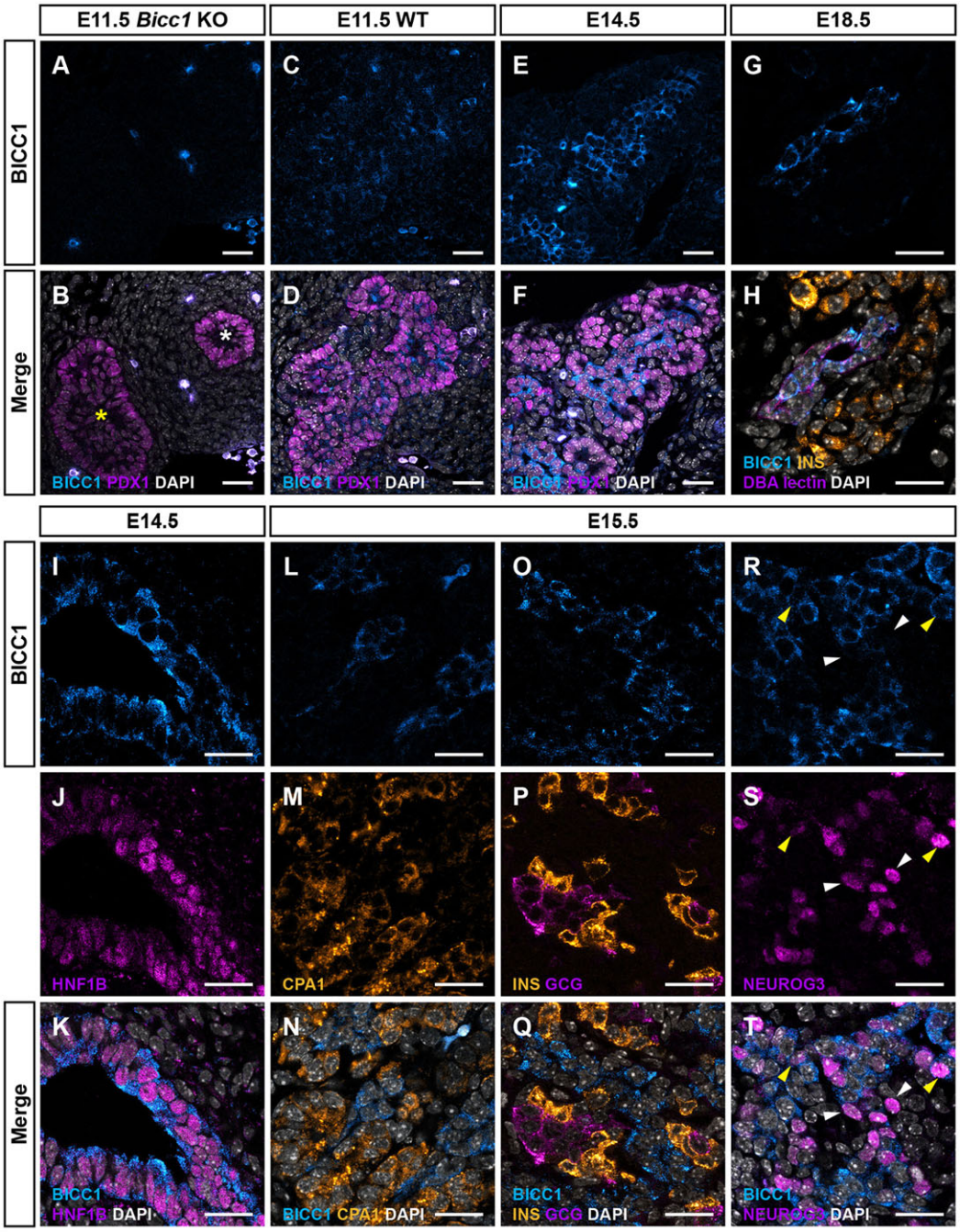

Fig. 1. BICC1 expression is restricted to the progenitors and ducts throughout pancreas development. Sections are stained by immunofluorescence and counterstained with DAPI (white). (A,B) Anti-BICC1 antibody specificity is assessed on E11.5 *Bicc1* KO pancreas. The pancreatic epithelium is highlighted by PDX1 (magenta, yellow asterisk), and no BICC1 signal is detected (cyan). (C,D) On the contrary, BICC1 immunoreactivity is weakly detected in WT pancreas at the same stage. (E,F) Its expression is stronger at E14.5. (G,H) It is also present at E18.5, in the duct highlighted by DBA lectin (magenta), but not in INS^+ cells (orange). (I-K) BICC1 expression domain colocalizes with HNF1B expression domain (magenta) at E14.5, (L,M) but is excluded from the acinar cells stained by CPA1 (orange) at E15.5. (O-Q) It is also excluded from the beta cells expressing INS (orange) and the alpha cells expressing GCG (magenta) at E15.5. (R-T) Part of $NEUROG3^+$ cells (magenta) are positive for BICC1 (yellow arrowheads), whereas the others are negative (white arrowheads). Scale bars: 25 µm in A-F; 20 µm in G-T.

pancreatic progenitors marked with PDX1 was not changed (Fig. 4H). Conversely, the endocrine progenitor number was significantly decreased by 34% in *Bicc1* KOs at the same stage (Fig. 4I-Q). It was consistent with a 30% decrease of *Neurog3* mRNA observed by qPCR at the same stage (supplementary material Fig. S4A). These results suggest that endocrine progenitor deficiency causes the observed endocrine cell decrease.

The decrease in $NEUROG3^+$ endocrine progenitors might be explained by a proliferation rate decrease, cell death or a generation rate reduction. It has already been shown that these cells hardly divide (Desgraz and Herrera, 2009). However, no $NEUROG3^+$ cells were positive for active caspase3 (active $CASP3^+$) or TUNEL in *Bicc1* KO E14.5 pancreas, indicating that there was no cell death (Fig. 4E-G; data not shown). These

Development (2015) 142, 858-870 doi:10.1242/dev.114611

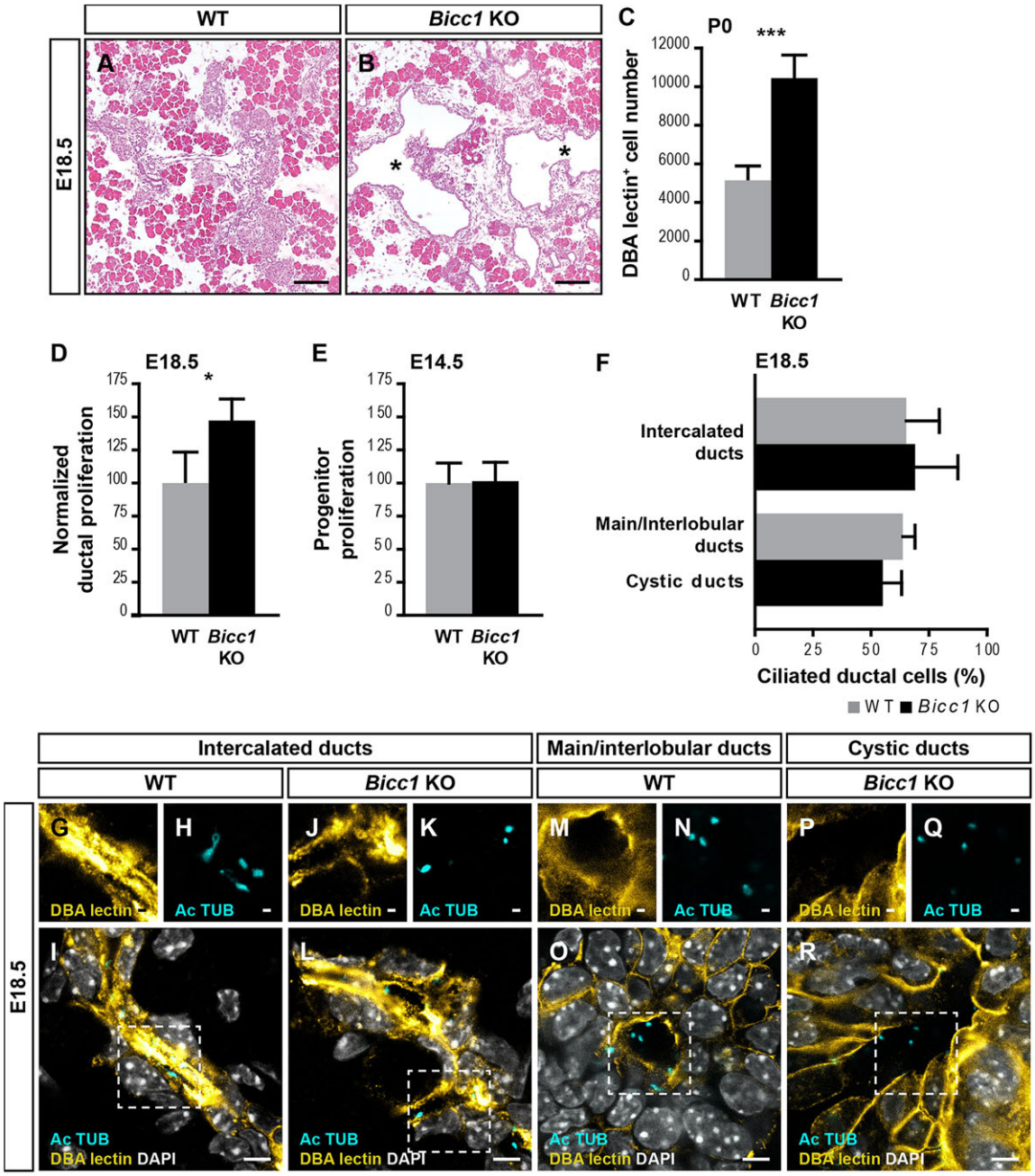

Fig. 2. Bicc1 KOs harbor pancreatic cysts caused by overproliferating ductal cells. (A,B) H&E staining of E18.5 WT and *Bicc1* KO pancreatic sections show cysts delineated by ductal cells in KO pancreata (asterisks). (C) Quantification of pancreatic DBA lectin$^+$ ductal cell number detected on immunofluorescence-stained sections at P0 shows that there are twice more ductal cells in *Bicc1* KO (n=4) than in WT (n=4, P=0.0003). (D) Percentage of DBA rhodamin$^+$ cells expressing MKI67, also known as Ki67, among the DBA rhodamin$^+$ ductal cells detected on immunofluorescence-stained sections; proliferation in *Bicc1* KO is increased 1.47-fold compared with WT. KO data are normalized to WT pancreas from the same background (WT, n=4; *Bicc1* KO, n=4; P=0.016). (E) Percentage of PDX1$^+$ pancreatic progenitor expressing PHH3 among the E14.5 pancreatic progenitors detected on immunofluorescence-stained sections. Proliferation is not affected in *Bicc1* KO (WT, n=4; *Bicc1* KO, n=3; P=0.9). Results are expressed as percentage of WT mean. (F) Percentage of DBA lectin$^+$ Ac TUB$^+$ cells among DBA lectin$^+$ ductal cells in intercalated and main/interlobular ducts in *Bicc1* KO and WT E18.5 pancreas quantified on three-dimensional (3D) reconstructed images. Cilia are not affected by *Bicc1* deletion (n=4 for both genotypes: intercalated ducts, P=0.75; main/interlobular ducts versus cystic ducts, P=0.12). (G-R) Cilia on ductal cells are detected by immunofluorescence for acetylated tubulin (Ac TUB) (cyan) and DBA lectin (yellow) on E18.5 pancreatic sections. Insets show higher magnification views of the dashed areas in two separate channels. Cilia are present in both WT and *Bicc1* KO pancreata in intercalated ducts and main/interlobular ducts as shown on optical section. Sections are counterstained with DAPI (white). Scale bars: 100 µm in A,B; 1 µm in G,H,J,K,M,N and P,Q; 5 µm in I,L,O and R. See supplementary material Table S1 for further data.

results suggest that NEUROG3$^+$ endocrine progenitor production is affected by *Bicc1* deletion.

To investigate possible additional differentiation defects after endocrine progenitors had been produced, a short-term lineage-tracing experiment was performed using the Neurog3-RFP reporter line (Y.H.K., unpublished) that marked NEUROG3 expression for about 48 h after their emergence. It enabled us to follow the differentiation path from endocrine progenitors toward endocrine

Development (2015) 142, 858-870 doi:10.1242/dev.114611

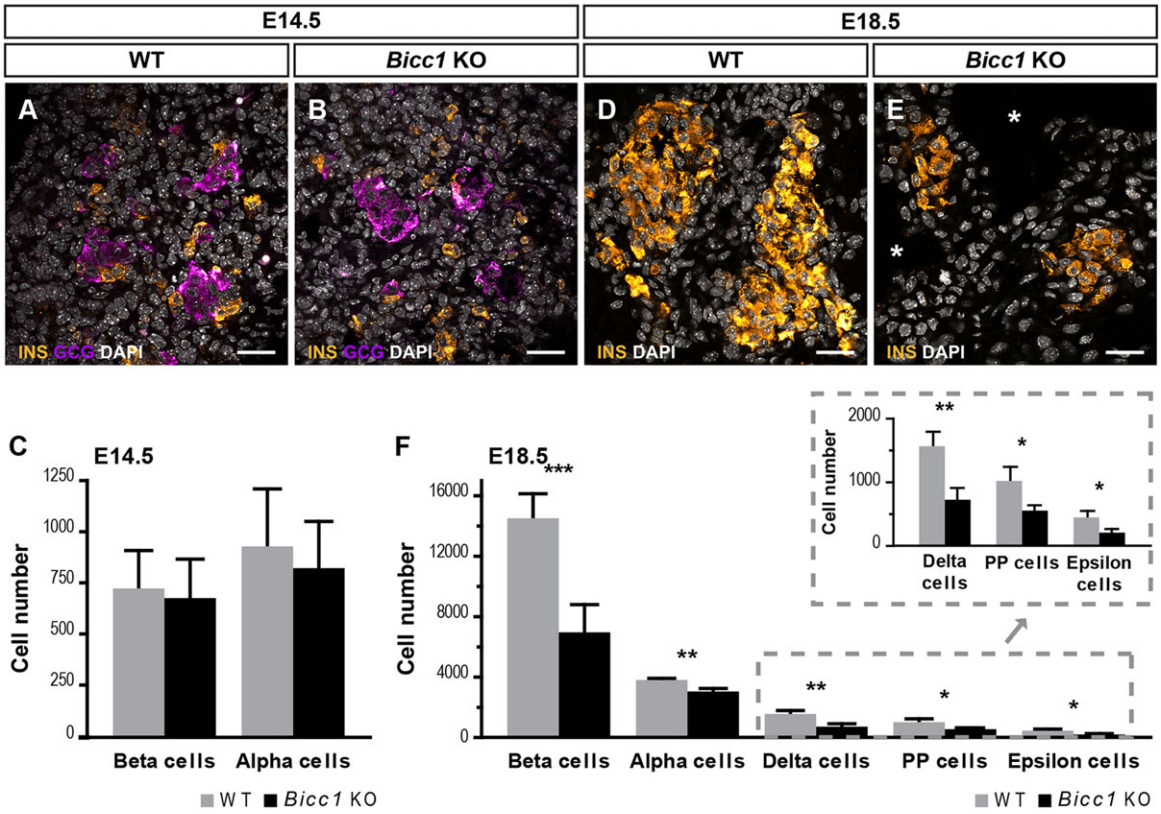

Fig. 3. Endocrine cells are decreased by Bicc1 deletion after E14.5. (A,B) Immunofluorescence staining highlighting GCG$^+$ alpha cells (magenta) and INS$^+$ beta cells (orange) in E14.5 *Bicc1* KO and WT pancreatic sections. (C) Quantification of INS$^+$ and GCG$^+$ cell number on the previous immunostainings shows no difference between *Bicc1* KO (INS$^+$ cells, n=4; GCG$^+$ cells, n=3) and WT (INS$^+$ cells, n=4, P=0.74; GCG$^+$ cells, n=4, P=0.62). (D,E) Immunofluorescence staining for INS (orange) on E18.5 *Bicc1* KO and WT pancreatic sections reveals a marked decrease in the KO sections. White asterisks indicate cysts. (F) Quantification of INS$^+$ beta cell, SST$^+$ delta cell, PP$^+$ PP cell and GHRL$^+$ epsilon cell numbers on E18.5 WT and *Bicc1* KO pancreatic sections reveals about 50% decrease (beta cells: n=4 for both genotype, P=0.0008; delta cells: WT, n=3; *Bicc1* KO, n=4, P=0.0029; PP cells: WT, n=3; *Bicc1* KO, n=4, P=0.012; epsilon cells: WT, n=3; *Bicc1* KO, n=4, P=0.011), whereas GCG$^+$ alpha cell number is reduced by 20% (WT, n=3; *Bicc1* KO, n=4, P=0.0024). Sections are counterstained with DAPI (white). Scale bars: 25 µm. See supplementary material Table S1 for further data.

cells. Indeed, cells started to express NEUROG3 before expressing RFP. They then switched off NEUROG3, whereas RFP expression was switched off only after they became hormone-positive. To quantitatively follow this differentiation pipeline, different cell populations were quantified: NEUROG3$^+$RFP$^-$, NEUROG3$^+$RFP$^+$, NEUROG3$^-$INS$^-$GCG$^-$RFP$^+$ and INS$^+$ or GCG$^+$RFP$^+$. All of these populations were decreased in *Bicc1* KO pancreata at E14.5 (Fig. 4I-Q). The similar ratio of the different populations in the *Bicc1* KO compared with control suggests that the decrease of endocrine cells is mainly due to a decreased conversion of bipotent progenitors into endocrine progenitors that normally differentiate thereafter (supplementary material Fig. S4B). Moreover, long-term lineage tracing using a Neurog3-Cre line crossed with Rosa26-YFP addressed whether NEUROG3$^+$ cell differentiation was steadily defective until the end of gestation. The total number of recombined cells harboring the reporter was reduced to the same extent as the endocrine cells, thus showing that the defect in endocrine progenitor cell production is sustained over the developmental period. No increase of NEUROG3 progeny in the acinar and ductal exocrine compartment was observed in *Bicc1* KOs, indicating that the cells expressing *Neurog3* are not diverted to a different developmental path (supplementary material Fig. S4C-O). Together, these data support the notion that the endocrine cell defect observed in *Bicc1* KOs is due to an endocrine progenitor generation defect.

BICC1 does not control SOX9, ONECUT1, FOXA2, PDX1, HNF1B or the NOTCH pathway but functions downstream of ONECUT1

The mechanism by which BICC1 controls NEUROG3$^+$ endocrine progenitors was further investigated. BICC1 binds to mRNAs and regulates positively or negatively their translation (Tran et al., 2010; Piazzon et al., 2012). A direct regulation of *Neurog3* mRNA by BICC1 is unlikely, as *Neurog3* transcriptional reporters were affected by *Bicc1* deletion to the same extent as NEUROG3 protein. Instead, BICC1 might target activators or repressors of *Neurog3*. NEUROG3$^+$ cell production is negatively regulated by the NOTCH pathway. HES1, expressed upon NOTCH pathway activation, is a repressor of *Neurog3*. Its deletion leads to massive NEUROG3$^+$ cell production and endocrine differentiation (Jensen et al., 2000; Lee et al., 2001). However, HES1 protein levels were not changed in *Bicc1* KO pancreata at E15.5 (Fig. 5A,B). Its mRNA level was also unchanged one day earlier, as was the mRNA level of Delta-like1 (*Dll1*) that activates the NOTCH pathway (Apelqvist et al., 1999) (Fig. 5C). We therefore tested whether the loss of *Bicc1* affects transcription factors that activate *Neurog3*, such as SOX9, FOXA2, PDX1, HNF1B or ONECUT1 (Jacquemin et al., 2000; Lynn et al., 2007). The SOX9 expression pattern was indistinguishable between *Bicc1* KO and WT pancreata at E14.5 (Fig. 5D,E). Moreover, the protein levels of SOX9, FOXA2, PDX1 and HNF1B were not changed at E15.5 upon *Bicc1* deletion

Development (2015) 142, 858-870 doi:10.1242/dev.114611

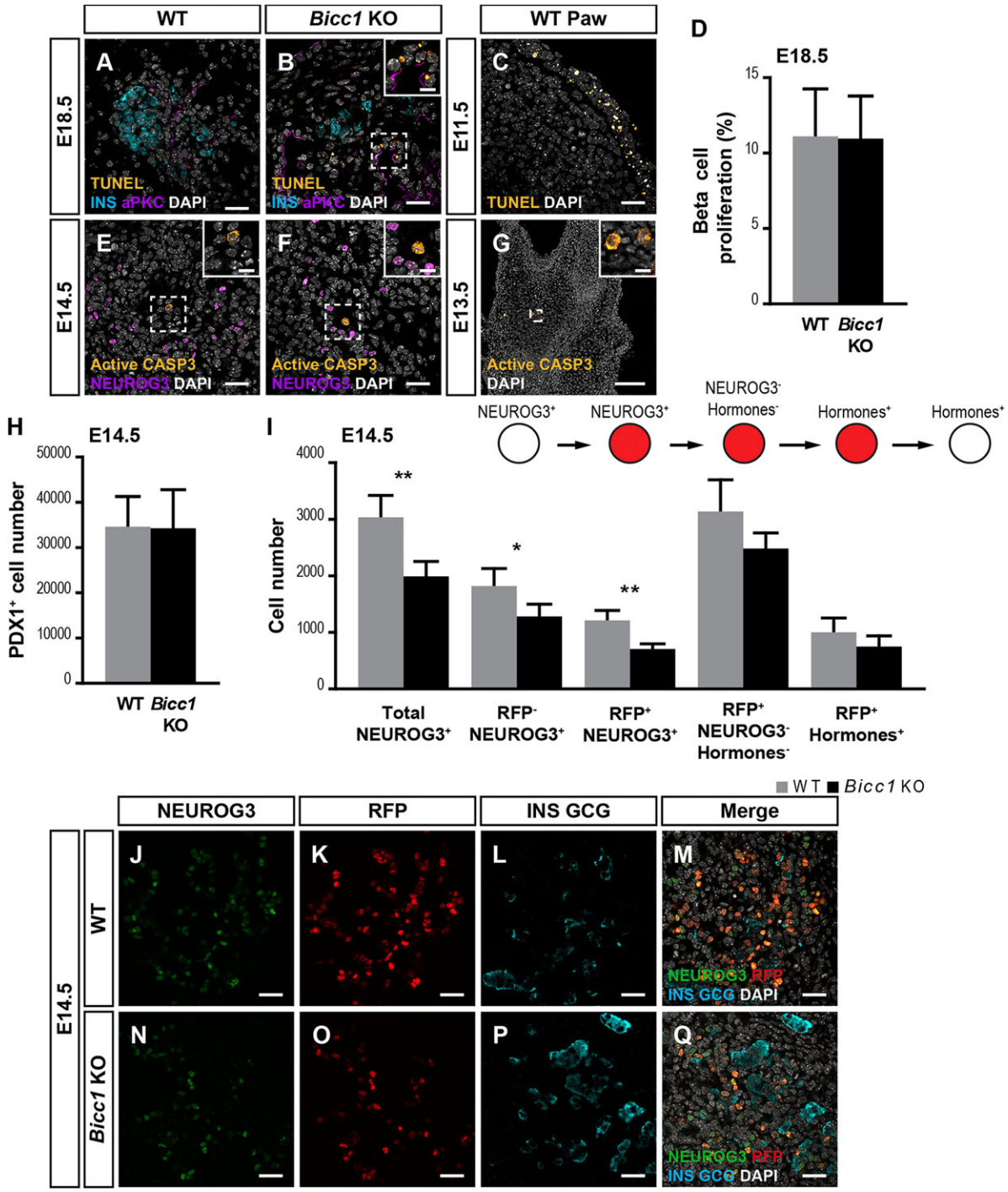

Fig. 4. Endocrine cell decrease is caused by endocrine progenitor generation defect. (A-C) TUNEL assay (orange) followed by immunofluorescence staining for INS (cyan) and aPKC, an apical marker (magenta), on E18.5 WT and *Bicc1* KO pancreatic sections shows no apoptotic death in INS$^+$ beta cells. By contrast, TUNEL$^+$ nuclei are seen in the duct delimited by aPKC in *Bicc1* KO pancreas. E11.5 paw is used as a positive control for the TUNEL assay. (D) Percentage of MKI67$^+$INS$^+$ beta cell number among beta cells quantified on immunostained sections shows no difference between E18.5 WT and *Bicc1* KO pancreata (P=0.95). (E-G) Immunofluorescence staining for active caspase3 (CASP3) (orange) and NEUROG3 (magenta) was performed on E14.5 WT and *Bicc1* KO pancreatic sections. Insets show a magnified view of the dashed area. No apoptosis is observed in endocrine progenitor cells. E13.5 paw is used as a positive control for active CASP3. (H) Quantification of the number of pancreatic progenitors immunoreactive for PDX1 on E14.5 pancreatic sections shows no difference between WT and *Bicc1* KO pancreata (P=0.95). (I-Q) An RFP reporter under *Neurog3* promoter, Neurog3-RFP, was used to characterize the differentiation flux from NEUROG3$^+$ endocrine progenitors toward hormone$^+$ endocrine cells. Cells are first NEUROG3$^+$ (green) before becoming double positive for NEUROG3 and RFP (red). They switch off NEUROG3 and thereafter start to express hormones, INS or GCG (cyan), before switching off RFP, as exemplified in the immunofluorescence staining on sections at E14.5 in WT and *Bicc1* KO pancreas. (I) Quantification of the different cell populations on sections reveals a global 34% decrease of the NEUROG3$^+$ endocrine progenitors in *Bicc1* KO pancreata (P=0.0043), corresponding to the decrease observed in both its RFP$^-$ and RFP$^+$ fractions (NEUROG3$^+$RFP$^-$, P=0.029; NEUROG3$^+$RFP$^+$, P=0.0021). The two last populations, NEUROG3$^-$Hormone$^-$RFP$^+$ cells and Neurog3$^-$Hormone$^+$RFP$^+$ cells, have a tendency to decrease that do not reach significance (Neurog3$^-$Hormones$^-$RFP$^+$ cells, P=0.08; Neurog3$^-$Hormones$^+$RFP$^+$ cells, P=0.16). Sections are counterstained with DAPI (white). For all experiments shown, n=4 for both genotypes. Scale bars: 25 µm in A-C,E,F and J-Q; 100 µm in G; 10 µm in insets. See supplementary material Table S1 for further data.

Development (2015) 142, 858-870 doi:10.1242/dev.114611

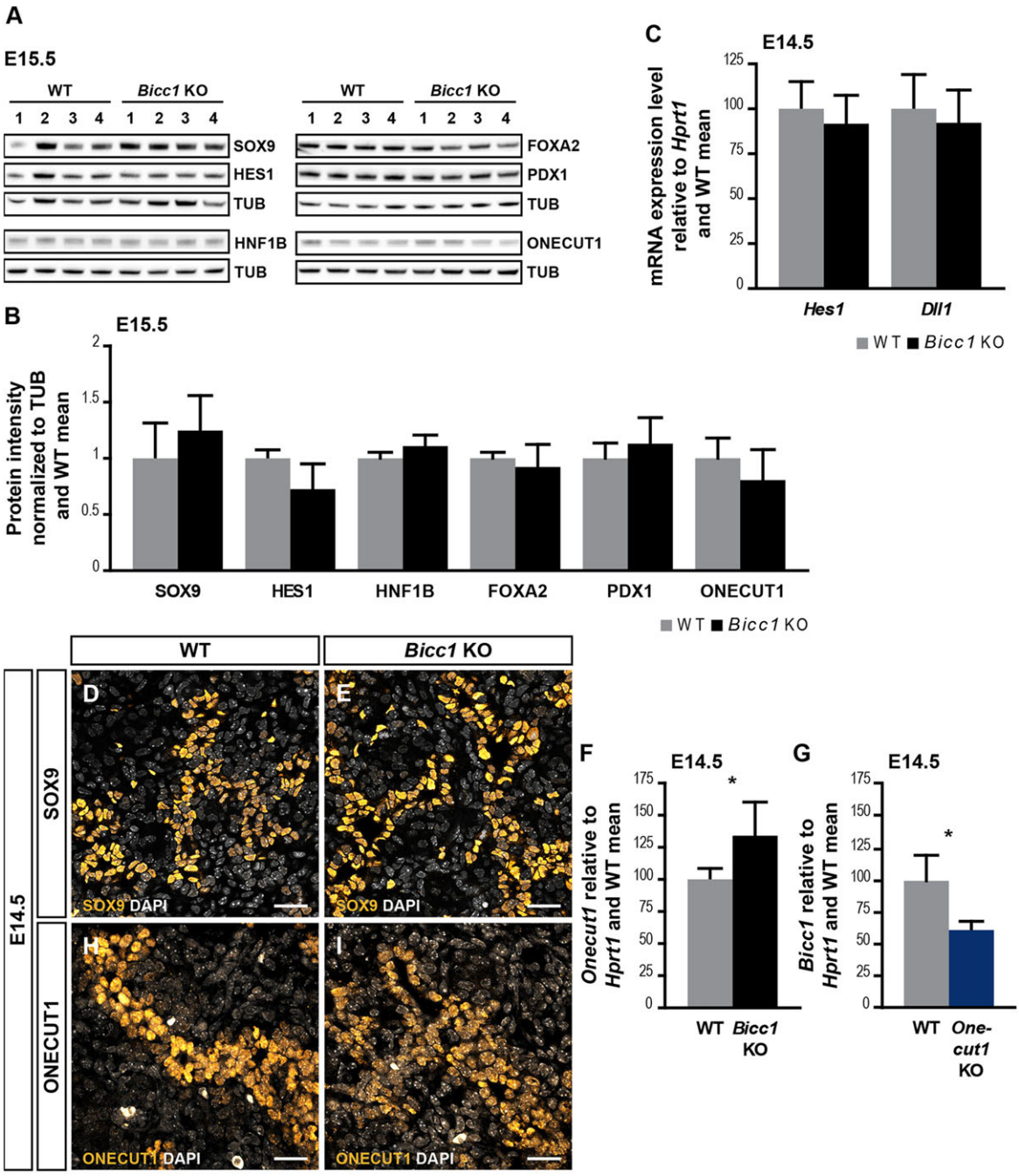

Fig. 5. BICC1 does not regulate the NOTCH pathway or known *Neurog3* transcriptional activators and functions downstream of ONECUT1. (A) Western blot performed for SOX9, HES1, HNF1B, FOXA2, PDX1 and ONECUT1 on E15.5 WT and *Bicc1* KO pancreata, and α-tubulin (TUB) as a loading control. (B) Quantification of the western blot shown in A is performed by normalizing band intensity to TUB intensity. Results are relative to WT mean. None of them are affected by *Bicc1* deletion (SOX9: WT, *n*=4; *Bicc1* KO, *n*=4, *P*=0.30; HES1: WT, *n*=4; *Bicc1* KO, *n*=4, *P*=0.06; HNF1B: WT, *n*=4; *Bicc1* KO, *n*=4, *P*=0.10; FOXA2: WT, *n*=4; *Bicc1* KO, *n*=4, *P*=0.48; PDX1: WT, *n*=4; *Bicc1* KO, *n*=4, *P*=0.37; ONECUT1: WT, *n*=7; *Bicc1* KO, *n*=8, *P*=0.13). (C) qPCR analysis for *Hes1* and *Dll1* performed on E14.5 WT and *Bicc1* KO dorsal pancreata does not show any differences (*Hes1*: WT, *n*=4; *Bicc1* KO, *n*=5, *P*=0.45; *Dll1*: WT, *n*=4; *Bicc1* KO, *n*=5, *P*=0.55). (D,E) Immunofluorescence staining performed on E14.5 WT (*n*=4) and *Bicc*1 KO (*n*=4) pancreatic sections do not show SOX9 (orange) expression pattern differences between both genotypes. (F) qPCR analysis of *Onecut1* in WT versus *Bicc1* KO E14.5 dorsal buds reveals a 34% increase in *Onecut1* transcript in the KO (WT, *n*=4; *Bicc1* KO, *n*=5; *P*=0.042). (G) qPCR analysis of *Bicc1* in WT versus *Onecut1* KO E14.5 dorsal buds shows a decrease by 40% of *Bicc1* transcript in the *Onecut1* KO (WT, *n*=4; *Onecut1*, *n*=3; *P*=0.027). (H,I) Immunofluorescence staining for ONECUT1 on E14.5 WT (*n*=2) and *Bicc1* KO (*n*=2) pancreatic sections shows no expression pattern difference. qPCR results are normalized to the housekeeping gene *Hprt1*. Results are represented in percentage of WT mean. Sections are counterstained with DAPI (white). Scale bars: 25 µm. See supplementary material Table S1 for further data.

(Fig. 5A,B). Although *Onecut1* mRNA was increased by 34% in *Bicc1* KO compared with WT pancreas (Fig. 5F), its protein level was not changed (Fig. 5A,B), and the localization of the protein was normal (Fig. 5H,I). In conclusion, NEUROG3^{+} cell reduction is not due to a decrease of its activators SOX9, FOXA2, PDX1, HNF1B and ONECUT1 or to NOTCH pathway alteration.

Onecut1 KO embryos also develop pancreatic cysts combined with a decrease in endocrine cells due to defective endocrine

Development (2015) 142, 858-870 doi:10.1242/dev.114611

progenitor differentiation (Lynn et al., 2007). As the experiments above showed that BICC1 does not promote ONECUT1 expression, we investigated whether BICC1 functions downstream of *Onecut1*. Indeed, we found that *Bicc1* mRNA was decreased by 40% in *Onecut1* KO pancreata (Fig. 5G), suggesting that ONECUT1 promotes *Bicc1* expression.

Although BICC1 was previously shown to control Wnt signaling in the node and in a cell line reporter assay (Maisonneuve et al., 2009), we did not detect any change in *Axin2* and *Tcf7*, two Wnt targets, nor any alterations in the expression of the *Axin2-lacZ* reporter in the pancreata of *Bicc1* KOs at E14.5 (supplementary material Fig. S5).

Cyst formation is associated with PKD2 downregulation and immune cell infiltration

To decipher the molecular mechanisms underlying cyst formation in *Bicc1* KO pancreata, E13.5 *Bicc1* KO and WT pancreas transcriptomes were compared by RNA sequencing. At this stage, duct enlargement was not yet observed, allowing us to detect expression changes prior to cyst formation rather than as a consequence of it. Only few genes were significantly upregulated or downregulated with an FDR<0.05 (Tables 1 and 2). All upregulated genes were expressed at low levels, with an rpkm<1 in WT pancreata. Among the downregulated genes, *Pkd2* was decreased 1.9-fold in *Bicc1* KO compared with WT pancreata. PKD2 deficiency results in pancreas and kidney cyst formation (Wu et al., 2000; Chang et al., 2006). PKD2 was expressed in the pancreatic ducts and appeared more weakly expressed in *Bicc1* KO. Moreover, western blot revealed a 2.1-fold decrease in PKD2 protein levels in *Bicc1* KO pancreata at E15.5, suggesting that regulation of PKD2 by BICC1 operates before translation (Fig. 6A-D).

Due to the small number of differentially regulated genes, it was not possible to perform a gene ontology analysis. Nevertheless, an important proportion of both up- and downregulated genes were related to the immune system, such as *S100a8*, *S100a9*, *Crp* and *Cma1*, thereby arguing for an immune status change (Tables 1 and 2). To further investigate this observation, the number of cells stained for CD45, a pan-immune cell marker, was quantified in *Bicc1* KO and WT E14.5 pancreata. It revealed a twofold increase in the *Bicc1* KO (Fig. 6E-G), with their presence correlated with the extent of cysts. Many of these cells were macrophages expressing EMR1, also called F4/80 (Fig. 6H-K). Moreover, tissue surrounding the cysts at E18.5 also exhibited numerous $CD45^+$ cells and $EMR1^+$ cells. The cysts at this stage were also surrounded by smooth muscle $actin^+$ ($ACTA2^+$) cells, suggestive of fibroblast activation (Apte et al., 1999; Haber et al., 1999) (Fig. 6L-O). $ACTA2^+$ cells were only present at E14.5 in a subset of *Bicc1* KO pancreata (Fig. 6H-K), which suggests a secondary effect of cyst formation and/or of immune cell recruitment. In conclusion, cysts arose in a context of PKD2 decrease and immune cell infiltration with stromal reaction.

Table 1. Upregulated mRNA in E13.5 *Bicc1* KO pancreas

Gene symbol	WT mean (rpkm)	*Bicc1* KO mean (rpkm)	Fold change	FDR
Slc16a3	0.89	2.02	2.27	0.0049
Gm15745	0.16	6.51	41.82	0.0006
RP23-281E24.2	0.49	1.87	3.85	<0.0001
Cma1	0.38	2.23	5.84	0.0009
Six2	0.18	2.67	15.06	0.0004
Fam162b	0.22	1.05	4.77	<0.0001
Hdc	0.10	0.32	3.12	0.0446
Rpl30-ps5	0.09	0.28	3.24	0.0473
Myod1	0.09	0.67	7.14	<0.0001
Nkx2-5	0.06	0.46	7.83	0.0321
Mcpt4	0.01	0.22	16.23	<0.0001
1700023F06Rik	0.01	0.50	50.43	<0.0001

mRNAs found upregulated in *Bicc1* KO compared with WT pancreas are ordered according to NIA array analysis tool. The ranking is based on a combination of their expression level in read per kilobase per million (rpkm), their fold change and their FDR.

Table 2. Downregulated mRNA in E13.5 *Bicc1* KO pancreas

Gene symbol	WT mean (rpkm)	*Bicc1* KO mean (rpkm)	Fold change	FDR
Bicc1	19.12	4.43	4.31	<0.0001
S100a9	11.63	2.10	5.54	0.0083
Pah	16.42	4.78	3.43	0.0118
S100a8	7.10	1.26	5.62	0.0111
Calcr	16.85	8.74	1.93	<0.0001
2010107G23Rik	30.82	20.19	1.53	0.0321
Pkd2	10.57	5.63	1.88	0.0001
Crp	23.85	15.71	1.52	0.0092
4930533K18Rik	4.95	1.48	3.34	<0.0001
BC100530	3.07	0.50	6.10	0.0118
Slc5a9	2.30	1.22	1.88	0.0481
Cer1	2.19	1.03	2.13	0.009
Ngp	2.69	0.39	6.88	0.0027
Anxa9	1.13	0.41	2.77	0.0006
Gm5483	1.31	0.23	5.77	0.0004
Gm13305	0.84	0.23	3.66	<0.0001
Olfm4	1.48	0.19	7.83	0.0001
Il11ra2	0.41	0.06	7.22	<0.0001
Gm2002	0.49	0.02	26.95	<0.0001

mRNAs found downregulated in *Bicc1* compared with WT pancreas are ordered according to NIA array analysis tool. The ranking is based on a combination of their expression level in rpkm, their fold change and their FDR.

DISCUSSION

BICC1 integrates epithelial morphogenesis and differentiation

We show here that BICC1 integrates appropriate pancreatic ductal tree morphogenesis and differentiation of endocrine cells originating from the progenitor-lined ducts. The absence of BICC1 causes cysts in both pancreatic and liver ducts, in addition to kidney dysplasia (Maisonneuve et al., 2009; Tran et al., 2010). Moreover, we show that BICC1 normally potentiates $NEUROG3^+$ endocrine progenitor production, leading to endocrine cell reduction in *Bicc1* KO pancreata (Fig. 7). These defects occur relatively late in pancreas development: BICC1 expression is elevated at E12.5 in bipotent ducto-endocrine progenitors, and upon the loss of *Bicc1*, NEUROG3 is decreased at E14.5 (RNA and cell number) but not yet at E13.5 (RNA sequencing). Endocrine cell decrease follows, being detected at E18.5 but not yet at E14.5. Our long-term lineage tracing shows a sustained decrease of 30-50% of endocrine cell production from E14.5 onwards. Glucagon cell production is therefore less affected in the *Bicc1* KO, as they are produced in large numbers before E14.5 (Johansson et al., 2007). $Neurog3^+$ progeny were globally reduced to the same extent as endocrine cells, indicating that BICC1 does not control endocrine cell production downstream of *Neurog3*.

BICC1 targets mediating endocrine cell differentiation

BICC1 is either able to repress translation by facilitating miRNA binding (Piazzon et al., 2012) or to enhance translation by inhibiting miRNA activity, thus stabilizing protein levels of the targets more than RNA levels (Tran et al., 2010; Gamberi and Lasko, 2012). We ruled out that BICC1 directly regulates *Neurog3*

Development (2015) 142, 858-870 doi:10.1242/dev.114611

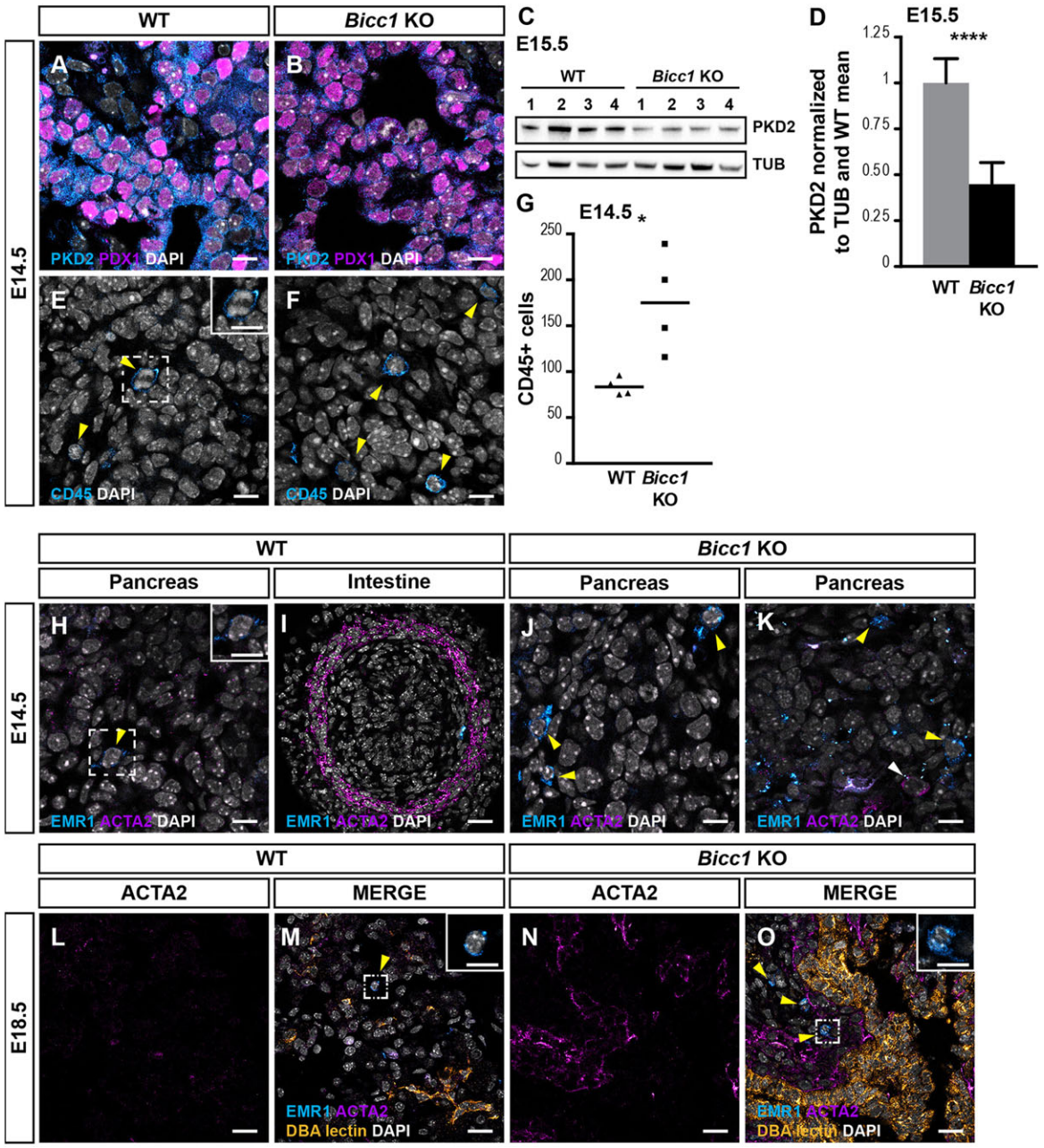

Fig. 6. PKD2 reduction and immune cell infiltration in *Bicc1* KO pancreas. (A,B) E14.5 WT and *Bicc1* KO pancreatic sections were stained by immunofluorescence for PKD2 (cyan) and PDX1 (magenta), highlighting pancreatic epithelium. E14.5 *Bicc1* KO pancreata (n=4) have a marked PKD2 decrease in the epithelium compared with WT littermate pancreata (n=4). (C) Western blot for PKD2 in E15.5 WT and *Bicc1* KO pancreata and TUB as a loading control. (D) Quantification of the western blot shown in C. PKD2 intensity is normalized to TUB intensity, and results are relative to WT mean. PKD2 in *Bicc1* KO pancreas is decreased 2.1-fold (WT, n=8; *Bicc1* KO, n=8; P<0.0001). (E,F) Immunofluorescence staining for CD45 (cyan), a pan-immune marker (yellow arrowheads), is performed on E14.5 WT and *Bicc1* KO pancreatic sections. Inset in E shows a high magnification of the dashed area. (G) Quantification of the immunostaining shows a 2.1-fold increase of $CD45^+$ cells in *Bicc1* KO (WT, n=4; *Bicc1* KO, n=4; P=0.017). (H-K) Immunofluorescence staining performed on E14.5 WT (n=5) and *Bicc1* KO (n=6) pancreata for EMR1 (cyan), a macrophage marker, and ACTA2 (magenta). E14.5 WT intestinal wall is used as a positive control for ACTA2. Both genotypes show $EMR1^+$ macrophages in the pancreas. Whereas $ACTA2^+$ cells are not observed in E14.5 WT pancreata, they were present in a subset of *Bicc1* KO pancreata. (L-O) Immunofluorescence staining for ACTA2 (magenta), EMR1 (cyan) and DBA lectin (orange) performed on E18.5 WT and *Bicc1* KO pancreatic sections. $ACTA2^+$ cells surround cysts (n=4), but not WT ducts (n=4). Macrophages (yellow arrowheads) are present around cystic ducts in E18.5 *Bicc1* KO pancreata (n=2), whereas there are only a few, scattered macrophages in WT pancreata (n=4). Insets show high magnification views of the dashed boxes. Sections are counterstained with DAPI (white). Scale bars: 10 µm in A,B,E,F and insets; 20 µm in H-O. See supplementary material Table S1 for further data.

stability or translation, as the reduction in number of cells expressing transcriptional reporters (Neurog3-Cre and Neurog3-RFP) is similar to the reduction in number of pro-endocrine cells expressing NEUROG3 protein. BICC1 might thus either enhance a transcriptional activator of *Neurog3* or inhibit a transcriptional repressor. HES1, a transcriptional repressor of *Neurog3*, was not changed in *Bicc1* KO pancreas, and neither were SOX9, FOXA2, PDX1 and HNF1B, some of its transcriptional activators (Lee et al.,

Development (2015) 142, 858-870 doi:10.1242/dev.114611

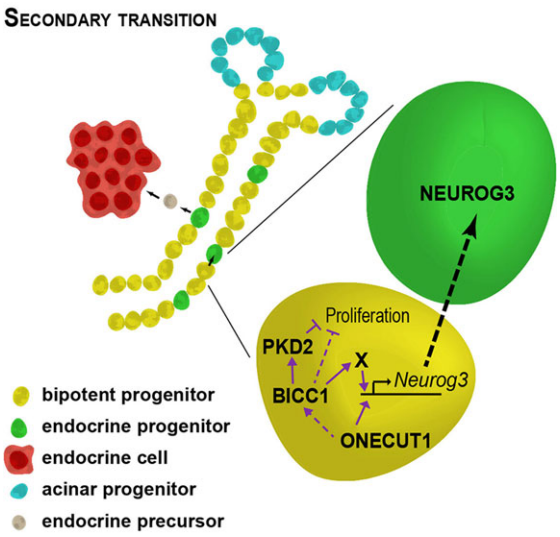

Fig. 7. Proposed model of BICC1 function during pancreas development. During the secondary transition, bipotent ductal progenitors (yellow) can differentiate into NEUROG3$^+$ endocrine progenitors (green). These progenitors leave the ducts (gray) while differentiating into endocrine cells (red). After the onset of the secondary transition, BICC1 is present in bipotent ductal progenitors (yellow). It regulates PKD2 and thereby inhibits ductal over-proliferation maintaining ductal homeostasis. BICC1 might also inhibit proliferation via other targets. It also promotes *Neurog3* expression via an unknown factor, enabling the differentiation toward endocrine progenitor (green). Whereas ONECUT1 directly activates *Neurog3* (Jacquemin et al., 2000), it also promotes *Bicc1* expression.

2001; Shih et al., 2012; Ejarque et al., 2013). ONECUT1 also activates *Neurog3* expression (Jacquemin et al., 2000), but although *Onecut1* was upregulated at the mRNA level, its protein level was unchanged, arguing against it being targeted by BICC1 (Fig. 7). Other transcription factors activate the *Neurog3* promoter, such as ONECUT2, HNF1A, GLIS3 and MYT1 (Lee et al., 2001; Vanhorenbeeck et al., 2007; Wang et al., 2007, 2008; Yang et al., 2011). It would thus be interesting to see whether these putative targets are affected by *Bicc1* deletion. The role of BICC1 in targeting mRNAs by miRNAs implies that its action is not seen at the mRNA level, as many miRNAs do not regulate transcript levels. It might explain why none of the genes above were changed in the transcriptome analysis of *Bicc1* KO versus WT pancreata. Few BICC1 targets are currently known, and the identification of its binding mRNA partners would give better insight into the generation of NEUROG3$^+$ endocrine progenitors.

BICC1 controls epithelial morphogenesis downstream of ONECUT1 and upstream of PKD2

Bicc1 KO pancreatic phenotype partially recapitulates the *Onecut1* KO phenotype. Indeed, in both cases, there are ductal cysts and fewer endocrine cells, due to a failure to produce endocrine progenitors (Jacquemin et al., 2000). We show that ONECUT1 controls *Bicc1* transcript levels. ONECUT1 might activate *Bicc1* expression directly, but an indirect control via HNF1B is plausible. Indeed, ONECUT1 enhances *Hnf1b* expression, and the latter is able to induce *Bicc1* expression in the kidney (Maestro et al., 2003; Verdeguer et al., 2010).

Cyst formation is a shared feature of several mutants affecting pancreas development. Cilia mutants have cysts in the pancreas, and *Onecut1* KOs lack cilia at early stages (Cano et al., 2004, 2006; Pierreux et al., 2006). However, the presence of cilia has been reported in the cochlea and node of *Bicc1* KOs (Maisonneuve et al., 2009; Piazzon et al., 2012), and we also observed them in their pancreata. However, BICC1 affects cilia position on the cells and their ability to synergistically rotate in the node. These cilia normally generate a flow of extracellular signals creating left-right asymmetry in embryos. In *Bicc1* KOs, the fluid flow randomization thus leads to left-right randomization (Maisonneuve et al., 2009). Their position and function is difficult to assess in the tortuous pancreatic ducts but is possibly altered.

Other mouse mutants also exhibit pancreatic cysts. *Neurog3* KOs harbor cysts smaller than those seen in *Bicc1* KOs (Magenheim et al., 2011). However, these cysts are thought to originate from an accumulation of endocrine progenitors failing to further differentiate, which is not the case in *Bicc1* KOs. It is also unlikely that the presence of cysts causes the endocrine defect, as certain gene KOs have normal endocrine cell numbers in spite of the presence of cysts (Cano et al., 2004, 2006). *Sox9* KO pancreata also have cysts due to an expanded ductal population, but SOX9 is not affected in *Bicc1* KOs. SOX9 and BICC1 appear to prevent cyst formation independently of each other by controlling *Pkd2* expression (Shih et al., 2012). *Pkd2* KO embryos and heterozygotes acquiring a spontaneous mutation of the second allele exhibit cysts in the pancreas and in the kidneys (Wu et al., 2000; Chang et al., 2006). In the kidneys, BICC1 inhibits targeting of *Pkd2* by miR-17, thus stabilizing PKD2 (Tran et al., 2010). PKD2 also functions downstream of BICC1 in osteoblasts, and knockdown of *Bicc1* is rescued by overexpressing *Pkd2* (Mesner et al., 2014). Together, these findings suggest that PKD2 is a major mediator of BICC1 activity in multiple organs.

An indirect and early mesenchymal contribution to cyst formation

A conserved feature of cyst formation in kidney is its association with fibrosis and infiltrating macrophages. Activated macrophages have been shown to promote cyst formation in polycystic kidney disease models (Karihaloo et al., 2011; Swenson-Fields et al., 2013; Ta et al., 2013). However, macrophage infiltration is insufficient to induce cyst formation in the fetal pancreas (Geutskens et al., 2005). In adults, however, macrophages are able to activate pancreatic stellate cells, the fibroblasts present in the pancreas (Schmid-Kotsas et al., 1999). Once activated, stellate cells start to express ACTA2 and promote fibrogenesis by producing extracellular matrix component (Masamune et al., 2009; Shi et al., 2014). In *Bicc1* KOs, the expansion of resident or infiltrating macrophages that we uncovered might promote cyst formation and at the same time activate stellate cells. Indeed, whereas immune cells were present in all pancreata as early as E14.5, ACTA2$^+$ cells were present in some *Bicc1* KO pancreata and became more prevalent at E18.5.

A role for BICC1 in syndromes associating kidney defects and diabetes?

Heterozygous *BICC1* mutations in human have been identified and associated with kidney dysplasia (Kraus et al., 2012). Other syndromes associate kidney defects with diabetes and/or pancreatic dysplasia. Indeed, MODY5 syndrome, in which *HNF1B* is mutated, is characterized by kidney cysts and diabetes (Bellanné-Chantelot et al., 2005). Both HNF1B and BICC1 prevent kidney cysts and control pancreas development, which might be explained by the ability of HFN1B to activate *Bicc1* directly (Haumaitre et al., 2006; Verdeguer et al., 2010) or indirectly (De Vas et al., 2015). It will be important to investigate whether *BICC1* mutations contribute to syndromes associated with kidney cysts and either diabetes or pancreatic

Development (2015) 142, 858-870 doi:10.1242/dev.114611

dysplasia or to link *BICC1* with already identified genes in such syndromes. Other monogenic forms of type 2 diabetes might also be associated with kidney dysplasia. For example, *GLIS3* mutations can cause neonatal diabetes associated with cystic kidneys (Senée et al., 2006). We have also observed a stromal reaction in *Bicc1* KOs, which leads us to think that some patients with Ivemark syndrome, who exhibit cystic kidneys and pancreatic fibrosis, might bear *Bicc1* mutations (Vankalakunti et al., 2007). The genetic causes of this familial syndrome have been identified in only a subset of cases, and include mutations in nephronophthisis 3 (*NPHP3*) (Bergmann et al., 2008; Fiskerstrand et al., 2010). These studies will be important for genetic counseling and patient management.

MATERIALS AND METHODS

Mice and genotyping

Mus musculus were either housed at EPFL, Switzerland, at the University of Copenhagen, Denmark, or at UCL, Belgium. The Service de la consommation et des affaires vétérinaires, Vaud in Switzerland, the Commission d'Ethique d'Expérimentation Animale of UCL in Belgium or the Dyreforsøgstilsynet in Denmark approved the mouse housing and experiments in their respective countries. Bicc1tm1Bdc (Bicc1) (Maisonneuve et al., 2009), Tg(Ngn3-tRFP)AGB (*Neurog3-RFP*) (Kim et al., unpublished data), Gt(ROSA)26Sortm1(EYFP)Cos (*Rosa YFP*) (Srinivas et al., 2001), Tg(Neurog3-cre)C1Able Ngn3-Cre (*Neurog3-Cre*) (Schonhoff et al., 2004) and *Onecut1* (Jacquemin et al., 2000) B6.129P2-Axin2tm1Wbm/J (*Axin2-lacZ*) (Lustig et al., 2002) mouse lines were used for this study. Genotyping primers and conditions are listed in supplementary material Table S2.

Specimen preparation

Guts, pancreas or dorsal pancreatic buds were dissected from mouse embryos at different stages or postnatally and treated as described by Cortijo et al. (2012). Cryostat sections (7 µm thick) were collected. For quantification, systematic uniform random-sampled sections (SUR sections) were collected every 5, 6 and 10 sections for E12.5, E14.5 and E18.5/P0, respectively.

Histology, immunofluorescence, X-Gal staining and TUNEL assay

Haematoxylin & eosin (H&E) staining was performed on cryosections. Immunofluorescence was performed as described by Cortijo et al. (2012). Antibodies and the dilution used in this study are listed in supplementary material Table S3. TUNEL assay was performed with an ApopTag fluorescein direct *in situ* apoptosis detection kit (Millipore, S7160) and followed by immunofluorescence staining as described by Cai et al. (2012). X-Gal staining was performed as described by Dessimoz et al. (2005).

Images and image analyses

A Leica SP8 confocal microscope, a Leica DM5500 upright wide-field microscope and a 3DHISTECH panoramic MIDI slide scanner were used for imaging. Quantifications were performed either manually or automatically by counting stained positive-cell profiles harboring a nucleus. See supplementary materials for an extended procedure description.

Western blot

E15.5 pancreata were lysed and sonicated in Laemmli buffer. After protein separation by electrophoresis and transfer, the membrane was incubated overnight with primary antibody. It was detected by chemiluminescence after HRP-conjugated secondary antibody incubation. Membranes were stripped and reprobed. See supplementary materials for an extended protocol. Antibodies and the dilution used in this study are listed in supplementary material Table S3. For comparison, the protein of interest was normalized to α-tubulin (TUB) level. Results are relative to WT mean.

RNA extraction and RT-qPCR

RNA was extracted from E10.5, E11.5, E12.5 and E14.5 dorsal bud using RNeasy Mini Kit (QIAGEN, 74104) including a DNase treatment with RNase-free DNase (QIAGEN, 79254) following the manufacturer instructions. 100 ng to 500 ng of RNA was then reverse-transcribed into cDNA with SuperScript III reverse transcriptase (Life Technologies, 18080-044) following the manufacturer's protocol. qPCRs were performed on 1/5 to 1/50 of the synthetized cDNA on the StepOnePlus real-time PCR system (Life Technologies) using Power SYBR Green as dye (Applied Biosystems, 4368577) and analyzed as described in Thompson et al. (2012). For comparison, the gene of interest was normalized to the housekeeping gene *Hprt1*. Results are indicated as percentage of the WT mean. Primer sequences and annealing temperatures are listed in supplementary material Table S2.

RNA sequencing

RNA was extracted from E13.5 dorsal bud using an RNeasy plus micro kit (QIAGEN, 74034) following the manufacturer protocol allowing small RNA elution. Three samples of the same genotype were then pooled together. TruSeqRNA libraries were synthetized from 500 ng of three WT and three *Bicc1* KO pools. Libraries were sequenced on an Illumina HiSeq 2000 platform (three replicates per condition, 100 nt single-end reads) and mapped to the mm9 mouse genome with bowtie v0.12.7 (480 million reads mapped in total) (Langmead et al., 2009). The data were then filtered to eliminate genes which had read per kilobase per million (rpkm) below 0.01, and were analyzed using the NIA array analysis tool (http://lgsun.grc.nia.nih.gov/ANOVA/). Differences with an FDR<0.05 were considered statistically significant. RNA sequencing data are available on NCBI Gene Expression Omnibus (accession number: GSE58833).

Statistical analysis

Statistical analyses were performed with GraphPad Prism4 and 6 software packages and Microsoft Excel. Results were indicated by the mean±s.d. except for Fig. 6G, which shows a dot plot with the mean. Differences assessed with *t*-test (assuming normal distribution) were considered statistically significant when the *P*-value was <0.05.

Acknowledgements

The authors would like to thank A. Sharov for his contribution to RNA sequencing data analysis and W. Hamilton for his comments on the manuscript. They also thank the group of J. Brickman, the group of P. Serup and the group of H. Semb for reagents.

Competing interests

The authors declare no competing or financial interests.

Author contributions

L.A.L. designed, carried out the experiments and wrote the manuscript. J.G. performed preliminary experiments analyzing the *Bicc1* KO phenotype and the OCT. Y.H.K. generated Neurog3-RFP mouse line. J.R. and S.C. analyzed the RNA sequencing data. P.J. collected *Onecut1* KO samples and their WT littermates. D.B.C. generated the Bicc1 mouse line. A.G.-B. designed the experiments and wrote the manuscript. All authors revised the manuscript.

Funding

This work has been supported by a Swiss National Fund Sinergia grant [CRSI33_130662] and a Novo Nordisk Found grant [nordic endocrinology 5099].

Supplementary material

Supplementary material available online at
http://dev.biologists.org/lookup/suppl/doi:10.1242/dev.114611/-/DC1

References

Apelqvist, Å., Li, H., Sommer, L., Beatus, P., Anderson, D. J., Honjo, T., Hrabě de Angelis, M., Lendahl, U. and Edlund, H. (1999). Notch signalling controls pancreatic cell differentiation. *Nature* **400**, 877-881.

Apte, M. V., Haber, P. S., Darby, S. J., Rodgers, S. C., McCaughan, G. W., Korsten, M. A., Pirola, R. C. and Wilson, J. S. (1999). Pancreatic stellate cells are activated by proinflammatory cytokines: implications for pancreatic fibrogenesis. *Gut* **44**, 534-541.

Ashcroft, F. M. and Rorsman, P. (2012). Diabetes mellitus and the β cell: the last ten years. *Cell* **148**, 1160-1171.

Barbacci, E., Reber, M., Ott, M., Breillat, C., Huetz, F. and Cereghini, S. (1999). Variant hepatocyte nuclear factor 1 is required for visceral endoderm specification. *Development* **126**, 4795-4805.

Bellanné-Chantelot, C., Clauin, S., Chauveau, D., Collin, P., Daumont, M., Douillard, C., Dubois-Laforgue, D., Dusselier, L., Gautier, J.-F., Jadoul, M. et al. (2005). Large genomic rearrangements in the hepatocyte nuclear factor-1beta (TCF2) gene are the most frequent cause of maturity-onset diabetes of the young type 5. *Diabetes* **54**, 3126-3132.

Bergmann, C., Fliegauf, M., Brüchle, N. O., Frank, V., Olbrich, H., Kirschner, J., Schermer, B., Schmedding, I., Kispert, A., Kränzlin, B. et al. (2008). Loss of nephrocystin-3 function can cause embryonic lethality, Meckel-Gruber-like syndrome, situs inversus, and renal-hepatic-pancreatic dysplasia. *Am. J. Hum. Genet.* **82**, 959-970.

Bingham, C. and Hattersley, A. T. (2004). Renal cysts and diabetes syndrome resulting from mutations in hepatocyte nuclear factor-1beta. *Nephrol. Dial. Transplant.* **19**, 2703-2708.

Cai, Q., Brissova, M., Reinert, R. B., Pan, F. C., Brahmachary, P., Jeansson, M., Shostak, A., Radhika, A., Poffenberger, G., Quaggin, S. E. et al. (2012). Enhanced expression of VEGF-A in β cells increases endothelial cell number but impairs islet morphogenesis and β cell proliferation. *Dev. Biol.* **367**, 40-54.

Cano, D. A., Murcia, N. S., Pazour, G. J. and Hebrok, M. (2004). Orpk mouse model of polycystic kidney disease reveals essential role of primary cilia in pancreatic tissue organization. *Development* **131**, 3457-3467.

Cano, D. A., Sekine, S. and Hebrok, M. (2006). Primary cilia deletion in pancreatic epithelial cells results in cyst formation and pancreatitis. *Gastroenterology* **131**, 1856-1869.

Chang, M. Y., Parker, E., Ibrahim, S., Shortland, J. R., Nahas, M. E., Haylor, J. L. and Ong, A. C. M. (2006). Haploinsufficiency of Pkd2 is associated with increased tubular cell proliferation and interstitial fibrosis in two murine Pkd2 models. *Nephrol. Dial. Transplant.* **21**, 2078-2084.

Cogswell, C., Price, S. J., Hou, X., Guay-Woodford, L. M., Flaherty, L. and Bryda, E. C. (2003). Positional cloning of jcpk/bpk locus of the mouse. *Mamm. Genome* **14**, 242-249.

Cortijo, C., Gouzi, M., Tissir, F. and Grapin-Botton, A. (2012). Planar cell polarity controls pancreatic beta cell differentiation and glucose homeostasis. *Cell Rep.* **2**, 1593-1606.

Desgraz, R. and Herrera, P. L. (2009). Pancreatic neurogenin 3-expressing cells are unipotent islet precursors. *Development* **136**, 3567-3574.

Dessimoz, J., Bonnard, C., Huelsken, J. and Grapin-Botton, A. (2005). Pancreas-specific deletion of beta-catenin reveals Wnt-dependent and Wnt-independent functions during development. *Curr. Biol.* **15**, 1677-1683.

De Vas, M. G., Kopp, J. L., Heliot, C., Sander, M., Cereghini, S. and Haumaitre, C. (2015). Hnf1b controls pancreas morphogenesis and generation of Ngn3+ endocrine progenitors. *Development* **142**, 871-882.

Ejarque, M., Cervantes, S., Pujadas, G., Tutusaus, A., Sanchez, L. and Gasa, R. (2013). Neurogenin3 cooperates with Foxa2 to autoactivate its own expression. *J. Biol. Chem.* **288**, 11705-11717.

Fiskerstrand, T., Houge, G., Sund, S., Scheie, D., Leh, S., Boman, H. and Knappskog, P. M. (2010). Identification of a gene for renal-hepatic-pancreatic dysplasia by microarray-based homozygosity mapping. *J. Mol. Diagn.* **12**, 125-131.

Flaherty, L., Bryda, E. C., Collins, D., Rudofsky, U. and Montogomery, J. C. (1995). New mouse model for polycystic kidney disease with both recessive and dominant gene effects. *Kidney Int.* **47**, 552-558.

Fossdal, R., Böðarsson, M., Ásmundsson, P., Ragnarsson, J., Peters, D., Breuning, M. H. and Jensson, O. (1993). Icelandic families with autosomal dominant polycystic kidney disease: families unlinked to chromosome 16p13.3 revealed by linkage analysis. *Hum. Genet.* **91**, 609-613.

Gamberi, C. and Lasko, P. (2012). The bic-C family of developmental translational regulators. *Comp. Funct. Genomics* **2012**, 141386.

Geutskens, S. B., Otonkoski, T., Pulkkinen, M.-A., Drexhage, H. A. and Leenen, P. J. M. (2005). Macrophages in the murine pancreas and their involvement in fetal endocrine development in vitro. *J. Leukoc. Biol.* **78**, 845-852.

Gradwohl, G., Dierich, A., LeMeur, M. and Guillemot, F. (2000). neurogenin3 is required for the development of the four endocrine cell lineages of the pancreas. *Proc. Natl. Acad. Sci. USA* **97**, 1607-1611.

Green, J. S., Parfrey, P. S., Harnett, J. D., Farid, N. R., Cramer, B. C., Johnson, G., Heath, O., McManamon, P. J., O'Leary, E. and Pryse-Phillips, W. (1989). The cardinal manifestations of Bardet-Biedl syndrome, a form of Laurence-Moon-Biedl syndrome. *N. Engl. J. Med.* **321**, 1002-1009.

Gresh, L., Fischer, E., Reimann, A., Tanguy, M., Garbay, S., Shao, X., Hiesberger, T., Fiette, L., Igarashi, P., Yaniv, M. et al. (2004). A transcriptional network in polycystic kidney disease. *EMBO J.* **23**, 1657-1668.

Gu, G., Dubauskaite, J. and Melton, D. A. (2002). Direct evidence for the pancreatic lineage: NGN3+ cells are islet progenitors and are distinct from duct progenitors. *Development* **129**, 2447-2457.

Haber, P. S., Keogh, G. W., Apte, M. V., Moran, C. S., Stewart, N. L., Crawford, D. H. G., Pirola, R. C., McCaughan, G. W., Ramm, G. A. and Wilson, J. S. (1999). Activation of pancreatic stellate cells in human and experimental pancreatic fibrosis. *Am. J. Pathol.* **155**, 1087-1095.

Harris, P. C. and Torres, V. E. (2009). Polycystic kidney disease. *Annu. Rev. Med.* **60**, 321-337.

Haumaitre, C., Barbacci, E., Jenny, M., Ott, M. O., Gradwohl, G. and Cereghini, S. (2005). Lack of TCF2/vHNF1 in mice leads to pancreas agenesis. *Proc. Natl. Acad. Sci. USA* **102**, 1490-1495.

Haumaitre, C., Fabre, M., Cormier, S., Baumann, C., Delezoide, A.-L. and Cereghini, S. (2006). Severe pancreas hypoplasia and multicystic renal dysplasia in two human fetuses carrying novel HNF1beta/MODY5 mutations. *Hum. Mol. Genet.* **15**, 2363-2375.

Horikawa, Y., Iwasaki, N., Hara, M., Furuta, H., Hinokio, Y., Cockburn, B. N., Lindner, T., Yamagata, K., Ogata, M., Tomonaga, O. et al. (1997). Mutation in hepatocyte nuclear factor-1 beta gene (TCF2) associated with MODY. *Nat. Genet.* **17**, 384-385.

Ivemark, B., Oldfelt, V. and Zetterstrom, R. (1959). Familial dysplasia of kidneys, liver and pancreas: a probably genetically determined syndrome. *Acta Paediatr.* **48**, 1-11.

Jacquemin, P., Durviaux, S. M., Jensen, J., Godfraind, C., Gradwohl, G., Guillemot, F., Madsen, O. D., Carmeliet, P., Dewerchin, M., Collen, D. et al. (2000). Transcription factor hepatocyte nuclear factor 6 regulates pancreatic endocrine cell differentiation and controls expression of the proendocrine gene ngn3. *Mol. Cell. Biol.* **20**, 4445-4454.

Jensen, J., Pedersen, E. E., Galante, P. P., Hald, J., Heller, R. S., Ishibashi, M., Kageyama, R., Guillemot, F., Serup, P. and Madsen, O. D. (2000). Control of endodermal endocrine development by Hes-1. *Nat. Genet.* **24**, 36-44.

Johansson, K. A., Dursun, U., Jordan, N., Gu, G., Beermann, F., Gradwohl, G. and Grapin-Botton, A. (2007). Temporal control of neurogenin3 activity in pancreas progenitors reveals competence windows for the generation of different endocrine cell types. *Dev. Cell* **12**, 457-465.

Kang, H. S., Kim, Y.-S., ZeRuth, G., Beak, J. Y., Gerrish, K., Kilic, G., Sosa-Pineda, B., Jensen, J., Foley, J., Jetten, A. M. (2009). Transcription factor Glis3, a novel critical player in the regulation of pancreatic beta-cell development and insulin gene expression. *Mol. Cell. Biol.* **29**, 6366-6379.

Karihaloo, A., Koraishy, F., Huen, S. C., Lee, Y., Merrick, D., Caplan, M. J., Somlo, S. and Cantley, L. G. (2011). Macrophages promote cyst growth in polycystic kidney disease. *J. Am. Soc. Nephrol.* **22**, 1809-1814.

Kesavan, G., Sand, F. W., Greiner, T. U., Johansson, J. K., Kobberup, S., Wu, X., Brakebusch, C. and Semb, H. (2009). Cdc42-mediated tubulogenesis controls cell specification. *Cell* **139**, 791-801.

Kousta, E., Hadjiathanasiou, C. G., Tolis, G. and Papathanasiou, A. (2009). Pleiotropic genetic syndromes with developmental abnormalities associated with obesity. *J. Pediatr. Endocrinol. Metab.* **22**, 581-592.

Kraus, M. R.-C., Clauin, S., Pfister, Y., Di Maïo, M., Ulinski, T., Constam, D., Bellanné-Chantelot, C. and Grapin-Botton, A. (2012). Two mutations in human BICC1 resulting in Wnt pathway hyperactivity associated with cystic renal dysplasia. *Hum. Mutat.* **33**, 86-90.

Langmead, B., Trapnell, C., Pop, M. and Salzberg, S. L. (2009). Ultrafast and memory-efficient alignment of short DNA sequences to the human genome. *Genome Biol.* **10**, pR25.

Lee, J. C., Smith, S. B., Watada, H., Lin, J., Scheel, D., Wang, J., Mirmira, R. G. and German, M. S. (2001). Regulation of the pancreatic pro-endocrine gene neurogenin3. *Diabetes* **50**, 928-936.

Lu, W., Peissel, B., Babakhanlou, H., Pavlova, A., Geng, L., Fan, X., Larson, C., Brent, G. and Zhou, J. (1997). Perinatal lethality with kidney and pancreas defects in mice with a targetted Pkd1 mutation. *Nat. Genet.* **17**, 179-181.

Lustig, B., Jerchow, B., Sachs, M., Weiler, S., Pietsch, T., Karsten, U., van de Wetering, M., Clevers, H., Schlag, P. M., Birchmeier, W. et al. (2002). Negative feedback loop of Wnt signaling through upregulation of conductin/axin2 in colorectal and liver tumors. *Mol. Cell. Biol.* **22**, 1184-1193.

Lynn, F. C., Smith, S. B., Wilson, M. E., Yang, K. Y., Nekrep, N. and German, M. S. (2007). Sox9 coordinates a transcriptional network in pancreatic progenitor cells. *Proc. Natl. Acad. Sci. USA* **104**, 10500-10505.

Maestro, M. A., Boj, S. F., Luco, R. F., Pierreux, C. E., Cabedo, J., Servitja, J. M., German, M. S., Rousseau, G. G., Lemaigre, F. P. and Ferrer, J. (2003). Hnf6 and Tcf2 (MODY5) are linked in a gene network operating in a precursor cell domain of the embryonic pancreas. *Hum. Mol. Genet.* **12**, 3307-3314.

Magenheim, J., Klein, A. M., Stanger, B. Z., Ashery-Padan, R., Sosa-Pineda, B., Gu, G. and Dor, Y. (2011). Ngn3(+) endocrine progenitor cells control the fate and morphogenesis of pancreatic ductal epithelium. *Dev. Biol.* **359**, 26-36.

Mahone, M., Saffman, E. E. and Lasko, P. F. (1995). Localized Bicaudal-C RNA encodes a protein containing a KH domain, the RNA binding motif of FMR1. *EMBO J.* **14**, 2043-2055.

Maisonneuve, C., Guilleret, I., Vick, P., Weber, T., Andre, P., Beyer, T., Blum, M. and Constam, D. B. (2009). Bicaudal C, a novel regulator of Dvl signaling abutting RNA-processing bodies, controls cilia orientation and leftward flow. *Development* **136**, 3019-3030.

Marshall, J. D., Bronson, R. T., Collin, G. B., Nordstrom, A. D., Maffei, P., Paisey, R. B., Carey, C., MacDermott, S., Russell-Eggitt, I., Shea, S. E. et al. (2005). New Alström syndrome phenotypes based on the evaluation of 182 cases. *Arch. Intern. Med.* **165**, 675-683.

Masamune, A., Watanabe, T., Kikuta, K. and Shimosegawa, T. (2009). Roles of pancreatic stellate cells in pancreatic inflammation and fibrosis. *Clin. Gastroenterol. Hepatol.* **7**, S48-S54.

Mesner, L. D., Ray, B., Hsu, Y.-H., Manichaikul, A., Lum, E., Bryda, E. C., Rich, S. S., Rosen, C. J., Criqui, M. H., Allison, M. et al. (2014). Bicc1 is a genetic determinant of osteoblastogenesis and bone mineral density. *J. Clin. Invest.* **124**, 2736-2749.

Nauta, J., Ozawa, Y., Sweeney, W. E., Rutledge, J. C. and Avner, E. D. (1993). Renal and biliary abnormalities in a new murine model of autosomal recessive polycystic kidney disease. *Pediatr. Nephrol.* **7**, 163-172.

Pan, F. C. and Wright, C. (2011). Pancreas organogenesis: from bud to plexus to gland. *Dev. Dyn.* **240**, 530-565.

Piazzon, N., Maisonneuve, C., Guilleret, I., Rotman, S. and Constam, D. B. (2012). Bicc1 links the regulation of cAMP signaling in polycystic kidneys to microRNA-induced gene silencing. *J. Mol. Cell Biol.* **4**, 398-408.

Pierreux, C. E., Poll, A. V., Kemp, C. R., Clotman, F., Maestro, M. A., Cordi, S., Ferrer, J., Leyns, L., Rousseau, G. G. and Lemaigre, F. P. (2006). The transcription factor hepatocyte nuclear factor-6 controls the development of pancreatic ducts in the mouse. *Gastroenterology* **130**, 532-541.

Reeders, S. T., Breuning, M. H., Davies, K. E., Nicholls, R. D., Jarman, A. P., Higgs, D. R., Pearson, P. L. and Weatherall, D. J. (1985). A highly polymorphic DNA marker linked to adult polycystic kidney disease on chromosome 16. *Nature* **317**, 542-544.

Rees, S., Kittikulsuth, W., Roos, K., Strait, K. A., Van Hoek, A. and Kohan, D. E (2014). Adenylyl Cyclase 6 deficiency ameliorates polycystic kidney disease. *J. Am. Soc. Nephrol.* **25**, 232-237.

Saffman, E., Styhler, S., Rother, K., Li, W., Richard, S. and Lasko, P. (1998). Premature translation of oskar in oocytes lacking the RNA-binding protein bicaudal-C. *Mol. Cell. Biol.* **18**, 4855-4862.

Schmid-Kotsas, A., Gross, H.-J., Menke, A., Weidenbach, H., Adler, G., Siech, M., Beger, H., Grünert, A. and Bachem, M. G. (1999). Lipopolysaccharide-activated macrophages stimulate the synthesis of collagen type I and C-fibronectin in cultured pancreatic stellate cells. *Am. J. Pathol.* **155**, 1749-1758.

Schonhoff, S. E., Giel-Moloney, M. and Leiter, A. B. (2004). Neurogenin 3-expressing progenitor cells in the gastrointestinal tract differentiate into both endocrine and non-endocrine cell types. *Dev. Biol.* **270**, 443-454.

Senée, V., Chelala, C., Duchatelet, S., Feng, D., Blanc, H., Cossec, J.-C., Charon, C., Nicolino, M., Boileau, P., Cavener, D. R. et al. (2006). Mutations in GLIS3 are responsible for a rare syndrome with neonatal diabetes mellitus and congenital hypothyroidism. *Nat. Genet.* **38**, 682-687.

Seymour, P. A., Shih, H. P., Patel, N. A., Freude, K. K., Xie, R., Lim, C. J. and Sander, M. (2012). A Sox9/Fgf feed-forward loop maintains pancreatic organ identity. *Development* **139**, 3363-3372.

Shi, C., Washington, M. K., Chaturvedi, R., Drosos, Y., Revetta, F. L., Weaver, C. J., Buzhardt, E., Yull, F. E., Blackwell, T. S., Sosa-Pineda, B. et al. (2014). Fibrogenesis in pancreatic cancer is a dynamic process regulated by macrophage-stellate cell interaction. *Lab. Invest.* **94**, 409-421.

Shih, H. P., Kopp, J. L., Sandhu, M., Dubois, C. L., Seymour, P. A., Grapin-Botton, A. and Sander, M. (2012). A Notch-dependent molecular circuitry initiates pancreatic endocrine and ductal cell differentiation. *Development* **139**, 2488-2499.

Srinivas, S., Watanabe, T., Lin, C.-S., William, C. M., Tanabe, Y., Jessell, T. M. and Costantini, F. (2001). Cre reporter strains produced by targeted insertion of EYFP and ECFP into the ROSA26 locus. *BMC Dev. Biol.* **1**, 4.

Swenson-Fields, K. I., Vivian, C. J., Salah, S. M., Peda, J. D., Davis, B. M., van Rooijen, N., Wallace, D. P. and Fields, T. A. (2013). Macrophages promote polycystic kidney disease progression. *Kidney Int.* **83**, 855-864.

Ta, M. H. T., Harris, D. C. H. and Rangan, G. K. (2013). Role of interstitial inflammation in the pathogenesis of polycystic kidney disease. *Nephrology (Carlton)* **18**, 317-330.

Taha, D., Barbar, M., Kanaan, H. and Williamson Balfe, J. (2003). Neonatal diabetes mellitus, congenital hypothyroidism, hepatic fibrosis, polycystic kidneys, and congenital glaucoma: a new autosomal recessive syndrome? *Am. J. Med. Genet. A* **122A**, 269-273.

Thompson, N., Gésina, E., Scheinert, P., Bucher, P. and Grapin-Botton, A. (2012). RNA profiling and chromatin immunoprecipitation-sequencing reveal that PTF1a stabilizes pancreas progenitor identity via the control of MNX1/HLXB9 and a network of other transcription factors. *Mol. Cell. Biol.* **32**, 1189-1199.

Tran, U., Zakin, L., Schweickert, A., Agrawal, R., Döger, R., Blum, M., De Robertis, E. M. and Wessely, O. (2010). The RNA-binding protein bicaudal C regulates polycystin 2 in the kidney by antagonizing miR-17 activity. *Development* **137**, 1107-1116.

Ulinski, T., Lescure, S., Beaufils, S., Guigonis, V., Decramer, S., Morin, D., Clauin, S., Deschênes, G., Bouissou, F., Bensman, A. et al. (2006). Renal phenotypes related to hepatocyte nuclear factor-1beta (TCF2) mutations in a pediatric cohort. *J. Am. Soc. Nephrol.* **17**, 497-503.

Vanhorenbeeck, V., Jenny, M., Cornut, J.-F., Gradwohl, G., Lemaigre, F. P., Rousseau, G. G. and Jacquemin, P. (2007). Role of the Onecut transcription factors in pancreas morphogenesis and in pancreatic and enteric endocrine differentiation. *Dev. Biol.* **305**, 685-694.

Vankalakunti, M., Gupta, K., Kakkar, N. and Das, A. (2007). Renal-hepatic-pancreatic dysplasia syndrome (Ivemark's syndrome). *Diagn. Pathol.* **2**, 24.

Verdeguer, F., Le Corre, S., Fischer, E., Callens, C., Garbay, S., Doyen, A., Igarashi, P., Terzi, F. and Pontoglio, M. (2010). A mitotic transcriptional switch in polycystic kidney disease. *Nat. Med.* **16**, 106-110.

Villiger, M., Goulley, J., Friedrich, M., Grapin-Botton, A., Meda, P., Lasser, T. and Leitgeb, R. A. (2009). In vivo imaging of murine endocrine islets of Langerhans with extended-focus optical coherence microscopy. *Diabetologia* **52**, 1599-1607.

Wang, S., Zhang, J., Zhao, A., Hipkens, S., Magnuson, M. A. and Gu, G. (2007). Loss of Myt1 function partially compromises endocrine islet cell differentiation and pancreatic physiological function in the mouse. *Mech. Dev.* **124**, 898-910.

Wang, S., Hecksher-Sorensen, J., Xu, Y., Zhao, A., Dor, Y., Rosenberg, L., Serup, P. and Gu, G. (2008). Myt1 and Ngn3 form a feed-forward expression loop to promote endocrine islet cell differentiation. *Dev. Biol.* **317**, 531-540.

Wessely, O., Tran, U., Zakin, L. and De Robertis, E. M. (2001). Identification and expression of the mammalian homologue of Bicaudal-C. *Mech. Dev.* **101**, 267-270.

Wu, G., Markowitz, G. S., Li, L., D'Agati, V. D., Factor, S. M., Geng, L., Tibara, S., Tuchman, J., Cai, Y., Park, J. H. et al. (2000). Cardiac defects and renal failure in mice with targeted mutations in Pkd2. *Nat. Genet.* **24**, 75-78.

Yang, Y., Chang, B. H.-J., Yechoor, V., Chen, W., Li, L., Tsai, M.-J. and Chan, L. (2011). The Krüppel-like zinc finger protein GLIS3 transactivates neurogenin 3 for proper fetal pancreatic islet differentiation in mice. *Diabetologia* **54**, 2595-2605.